Cyclen-based chelators for the inhibition of Aβ aggregation: Synthesis, anti-oxidant and aggregation evaluation.

Mahmoud El Safadi [a], Mohan Bhadbhade [b], Ronald Shimmon [a], Anthony T. Baker [c], Andrew M. McDonagh [a,*]

[a] School of Mathematical and Physical Sciences, University of Technology Sydney, Broadway, Ultimo, NSW 2007 Australia

[b] School of Chemistry, The University of New South Wales, Sydney, 2052, Australia

[c] College of Science, Health and Engineering, La Trobe University, Melbourne, 3086, Australia

Corresponding author email address: andrew.mcdonagh@uts.edu.au

Abstract: The aggregation of the protein amyloid-β in the brain has been associated with neurodegenerative diseases such as Alzheimer's disease. Such aggregation of amyloid-β can be induced by misregulated metal ions such as Cu^{2+} and Zn^{2+}. Here we present a series of four metal chelating compounds based on the cyclen macrocycle that bears pendant arms to provide additional anti-oxidant activity. The corresponding Cu^{2+}, Zn^{2+} and Ni^{2+} complexes have been synthesized and characterized to examine the ability of the chelators to bind to the metal centres. $Aβ_{40}$ de-aggregation by the cyclen compounds was assessed using turbidometry and the re-solubilization of the $Aβ_{40}$ was also examined. Our results show that the cyclen compounds have the ability to effectively chelate Cu^{2+} and Zn^{2+} metal ions and thus de-aggregate $Aβ_{40}$ that has been aggregated due to the presence of these ions. The antioxidant properties of the cyclen compounds was tested by using the DPPH scavenging assay and the results show that some of the compounds can decrease oxidative stress.

Introduction

Alzheimer's disease (AD) is a progressive illness that is often characterized by deposits of the peptide amyloid-β (Aβ), oxidative stress, and elevated levels of particular metal ions within regions of the brain [1-4]. Amyloid-β peptides are generally derived from amyloid precursor protein (APP) [5, 6], which is located on the cell membrane [7]. APP can be cleaved either by a non-amyloidogenic pathway yielding the soluble APPα, or by the amyloidogenic pathway, where β-secretase cleaves APP to give APPβ and the c99 terminal. The c99 is further cleaved to give amyloid β[5, 8, 9], which is normally degraded and escorted from the brain[10]. However, mis-regulated metal ions (zinc, copper, nickel, iron) can prevent the clearance of amyloid β proteins by blocking their passage through the blood brain barrier (BBB)[11]. At the same time, accumulated free metal ions can stimulate the production of extracellular amyloid β by binding the active site of α-secretase in APP thus favouring the amyloid pathway over the non-amyloid pathway. Subsequently, amyloid β may aggregate in the brain to form plaques [10].

Misregulated metal ions can also catalyze the production of reactive oxygen species (ROS) that induce oxidative stress in the brain [12]. The metals copper, zinc, and iron have been implicated in this regard and copper in particular has been proposed to have a cumulative effect that impairs processes that remove Aβ from the brain [10]. Currently, the role of Aβ and indeed that of the various metal ions and their interactions appears to be far from fully understood. Other factors such as neuroinflammation are currently receiving intense investigation [13] and quite recent work points to a connection between copper ions and the inflammatory response [14].

The binding and removal of excess metal species using metal chelating compounds, coupled with antioxidant activity to remove ROS, has been identified as a promising strategy to treat AD [15]. A number of metal chelators have been investigated as metal ion chelation

therapy agents [16, 17]. For example, desferrioxamine has a high affinity towards free iron [18] as well as Cu and Zn, with which it forms stable complexes that slow down the development of Alzheimer's disease [19]. 8-Hydroxyquinoline derivatives such as clioquinol have been tested. Clioquinol has a hydrophobic character and readily crosses the blood brain barrier (BBB) and can bind to Zn and Cu that are attached to Aβ. On the other hand, clioquinol-copper complexes can increase the level of biological copper in the brain and has been shown to redistribute copper ions [16, 20].

Macrocyclic polyamine compounds have a strong affinity for metals ions [21] and have found applications in diagnostic imaging, as therapeutic agents [22-24] and in targeting Aβ amyloid aggregation [25]. These compounds have important physical properties such as low molecular weights, neutral charge, amphiphilic solubility and low toxicities [22].
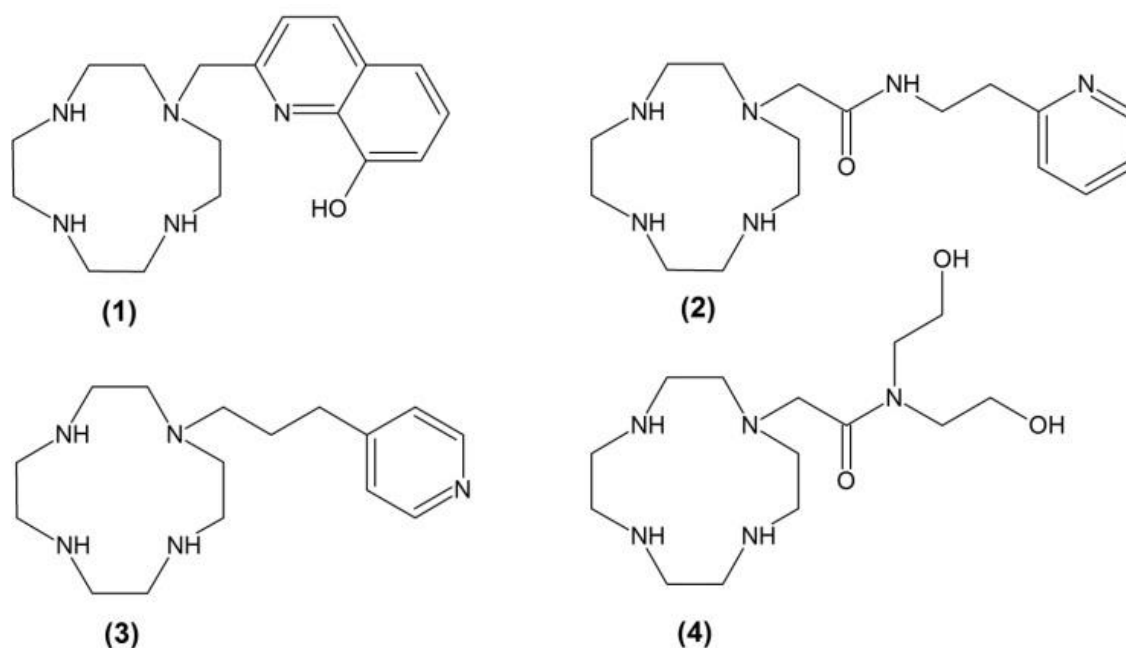

Fig. 1. Chemical structures of the chelators investigated in the current work.

In this work, cyclen-based chelators have been synthesized (Fig. 1) that bear pendant arms with redox properties that increase the lipophilicity of the resultant compounds and that may reduce the oxidative stress that is caused by particular metals ions. In compound **1**, the

phenolic hydroxyl moiety of the pendant 8-hydroxyquinoline group act as an antioxidant [26] while the quinolinyl moiety has been shown to decrease levels of Aβ in the brain of AD patients without affecting serum metal ion levels (Zn^{2+} and Cu^{2+}) [27]. The pendant arm of **2** (Fig. 1) bears a 2-(pyridin-2-yl)ethylacetamide group that may also increase lipophilicity and decrease oxidative stress. For comparison, compound **3**, which bears a propylpyridin-4-yl pendant arm should increase lipophilicity but have limited effect on oxidative stress. We predicted that the anti-oxidant activity of **4** would be similar to that of **2** but allows the effect of more polar substituents to be examined. We report here our findings describing the synthesis of compounds **1-4** and some X-ray structural determinations of complexes with Cu^{2+}, Zn^{2+}, and Ni^{2+}.

Results and Discussion
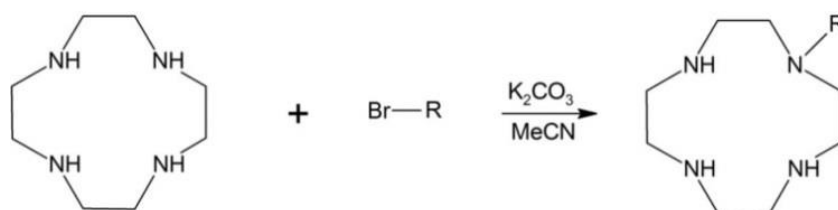
**Scheme 1.** Synthesis of **1-4** where R = pendant arm (see Figure 1).

The chelators, **1-4**, were synthesized by the reaction of 1,4,7,10-tetrazacyclododecane (cyclen) with the corresponding alkylbromide in a 2:1 (cyclen:RBr) molar ratio. Using this ratio, reasonable yields were obtained and the formation of di- and tri-substituted cyclen was minimized. The monosubstituted cyclen is significantly less reactive than unsubstituted cyclen and so only small amounts of di- and tri- substituted cyclen (~10% and ~3%, respectively) were obtained. The resultant mixtures could be readily separated using column chromatography. Attempts to protect three of the cyclen nitrogen atoms using $P(NMe_2)_3$ (and thus avoid multiple substitution products) [28] resulted in only very low yields and so this

method was not pursued further. The synthesis and characterization of compounds **1**, **3** and **4** has not been previously reported while **2** has been reported elsewhere [29].
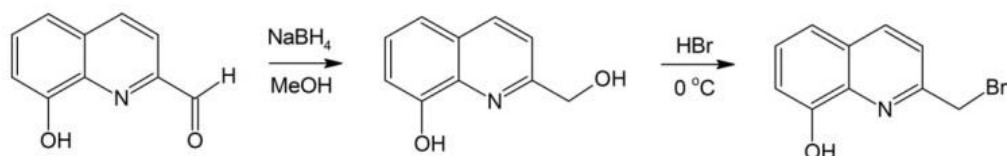
Scheme 2: Synthesis of 2-bromomethyl-8-hydroxyquinoline

The syntheses of the R-Br groups that subsequently form the pendant arms are shown in Schemes **2** and **3**. 2-Bromomethyl-8-hydroxyquinoline (Scheme 2) was synthesized in two steps from 2-formyl-8-hydroxyquinoline by first reducing the aldehyde to the corresponding alcohol followed by bromination of the alcohol using hydrobromic acid. 2-Bromo-N-(2-(pyridin-2-yl)ethyl)acetamide and bis(2-hydroxyethyl)carbamic bromide were prepared by reacting the commercially available amines with bromoacetyl bromide.
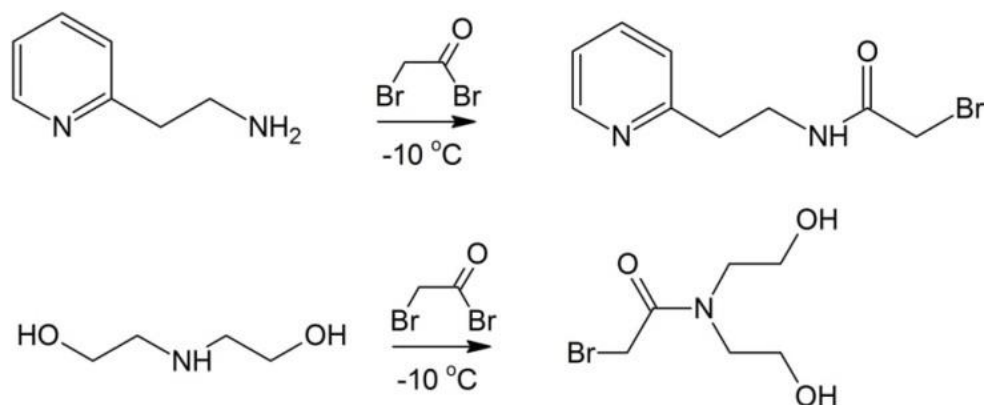
Scheme 3: Synthesis of 2-bromo-N-(2-(pyridin-2-yl)ethyl) acetamide and bis(2-hydroxyethyl)carbamic bromide

Metal complexes (Cu, Zn, and Ni) of 1-4 were synthesized by reaction of the substituted cyclen compounds with the corresponding metal salts (either sulfate or chloride) in methanol or water. The resultant complexes could be readily purified by recrystallization, which also gave some crystals suitable for structure determination by X-ray diffraction.
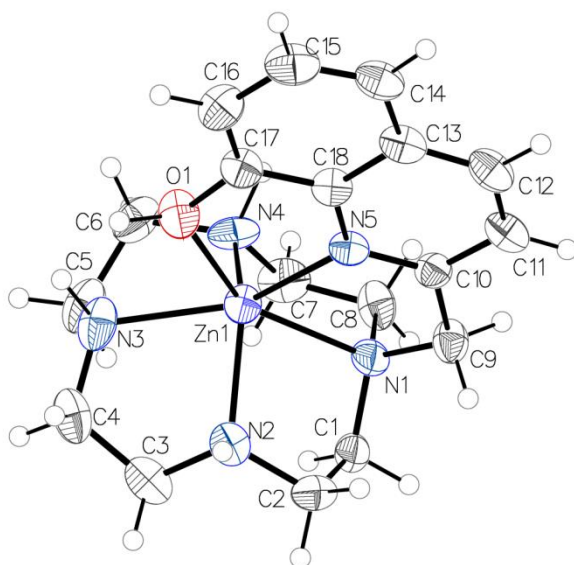
X-ray Crystallography

Fig. 2. ORTEP diagram showing the structure of the Zn-1 unit.Main Text Paragraph.

X-ray crystal structures were obtained for the complexes Cu-**2**, Cu-**3**, Zn-**1**, and Ni-**3**. An ORTEP diagram for Zn-**1** is shown in Figure 2. Table 1 shows selected bond lengths and angles for Zn-**1**, Cu-**2**, Cu-**3**, and Ni-**3**. Other crystal data are collected in the supporting information.

Table 1: Selected bond lengths and angles for Zn-**1**, Cu-**2**, Cu-**3**, and Ni-**3**.

	Zn-**1**	Cu-**2**	Cu-**3**	Ni-**3**
M-N1	2.304 (5)	2.055 (13)	2.047 (4)	2.143 (6)
M-N2	2.120 (5)	2.016 (12)	2.019 (4)	2.044 (7)
M-N3	2.211 (5)	2.024 (13)	2.022 (4)	2.113 (7)
M-N4	2.111 (5)	2.058 (11)	2.020 (4)	2.071 (7)
M-N5	2.094 (4)	-	-	-
M-O	2.340 (4)	2.108 (9)	2.138 (3)	2.099(5)
M-N1-C9	109.4 (3)	112.9 (9)	113.2 (3)	112.6 (5)
N1-C9-C10	112.3 (5)	116.4 (13)	115.3 (5)	118.0 (6)
N1-M-N2	80.26 (17)	85.6 (5)	86.61 (18)	84.9 (3)
N2-M-N3	79.87 (19)	86.6 (5)	85.91 (18)	84.3 (3)
N3-M-N4	80.4 (2)	86.7 (5)	85.99 (18)	81.4 (3)
N4-M-N1	79.78 (18)	86.4 (5)	86.58 (18)	82.0 (3)

In each of the structures, the cyclen macrocycle is bound to the metal centre in the expected tetradentate fashion. In the structure of Zn-**1**, the remaining two coordination sites of the distorted octahedral geometry are occupied by the donor atoms (N and O) of the 8-hydroxyquinolinyl pendant arm. Thus, this ligand binds in a hexadentate fashion. The charge of the Zn-**1** cation is balanced by a tetrahedral $ZnCl_4^{2-}$ anion (not shown).

The metal-nitrogen bond distances for Zn-**1** (Table 1) are generally longer than the metal-nitrogen distances for the other complexes. Similarly, the N-M-N angles for Zn-**1** are smaller than those the other complexes as are the M-N1-C9 and N1-C9-C10 angles. These geometries allow for accommodation of the bidentate quinolinyl group in the coordination sphere of the metal.

In the structures of Cu-**2**, Cu-**3** and Ni-**3**, the pendant arms of **2** and **3** are not coordinated to the metal centre. In the cases of Cu-**2** and Cu-**3**, an O atom of the sulfate anions occupies an apical position to give square pyramidal coordination geometry. In the case of Ni-**3**, there are two molecules in the asymmetric unit. Each complex has two water molecules coordinated to the Ni centre resulting in a distorted octahedral geometry and no coordination of the accompanying sulfate anions.

A turbidimetric assay [30] was used to investigate the effect of 1-4 on the Cu^{2+}-induced aggregation of $A\beta_{40}$. Aggregation of $A\beta_{40}$ was induced by the addition of Cu^{2+} ions. This was accompanied by a significant increase in optical absorbance, which was monitored at 405 nm. Upon addition of 1-4, disaggregation of $A\beta_{40}$ occurred with a corresponding decrease in optical absorbance as the turbid suspension of the $A\beta_{40}$ aggregates re-dissolved due to the withdrawal and binding of the Cu^{2+} ions by the chelators. Experimental data are presented in Figure 3. Each of the chelators was effective at decreasing turbidity to levels only marginally above that of un-aggregated $A\beta_{40}$. Within error, each of 1-4 exhibited the same effect on turbidity.
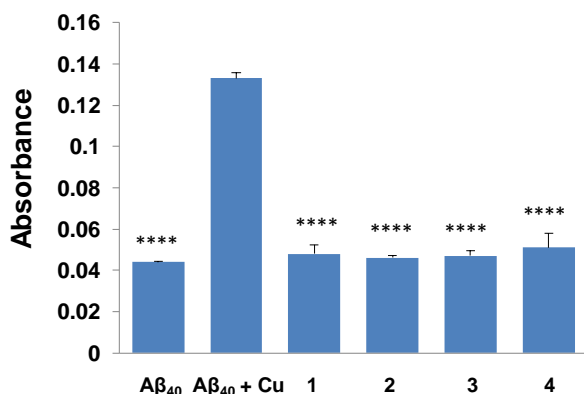
Fig. 3: Optical absorbance at 405 nm for $A\beta_{40}$, $A\beta_{40}$ + Cu, and $A\beta_{40}$ + Cu after incubation for 4 h with **1-4**. Different from control ($A\beta40$ + Cu): ****$P < 0.0001$
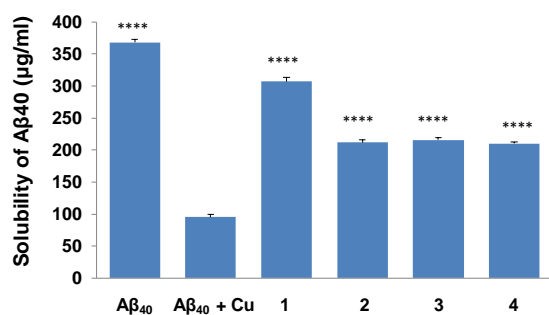
Fig. 4: Solubility data for $A\beta_{40}$, $A\beta_{40}$+ Cu^{2+} ions, and $A\beta_{40}$+ Cu^{2+} after incubation with **1-4** for 4h. Different from control ($A\beta40$ + Cu): ****$P < 0.0001$.

Table 2. ESI-MS data from analysis of the supernatant of centrifuged samples of $A\beta40$ after de-aggregation using 1-4.

Chelator	$[A\beta40 + 6H]^{6+}$ (m/z) ($C_{194}H_{301}N_{53}O_{58}S$)	$[A\beta40 + 5H]^{5+}$ (m/z) ($C_{194}H_{300}N_{53}O_{58}S$)	$[A\beta40 + 4H]^{4+}$ (m/z) ($C_{194}H_{299}N_{53}O_{58}S$)	Cu [Cyclen compound] (m/z)
1	722.5357	866.8405	1083.3023	391.1432 ($CuC_{18}H_{26}ON_5$)
2	722.5353	866.8414	1083.3010	397.1767 ($CuC_{17}H_{30}ON_6$)
3	722.5346	866.8401	1083.3013	353.1644 ($CuC_{16}H_{28}N_5$)
4	722.7002	866.8436	1083.3021	380.1725 ($CuC_{14}H_{31}O_3N_5$)

The effect of **1-4** on $A\beta_{40}$ aggregation was further evaluated using the BCA assay [31, 32], which assesses the concentration of $A\beta_{40}$ in solution. Figure 4 and Table S9 show solubility data for $A\beta_{40}$ before and after treatment with Cu^{2+} ions and then with **1-4.** After incubation for 48 hours with Cu^{2+} ions, the solubility of $A\beta_{40}$ decreased to ~25 % of the initial concentration due to Cu^{2+}-induced aggregation. Upon addition of **1-4**, the solubility increased significantly after incubation for 4 h. The re-solubilisation of the $A\beta_{40}$ is ascribed to copper sequestration by **1**-**4** to disassemble the aggregates and thus return the $A\beta_{40}$ to solution. Comparison of the four chelators reveals that treatment with **1** returns considerably more $A\beta_{40}$ to solution (~83% of the original material) than does **2-4** (58%, 59% and 57%, respectively). We propose that the enhanced chelating ability of **1** may be due to its hexadentate binding compared to the tetradentate nature of **2-4**. The UV-visible spectrum of Cu-**1** (Figure S13) exhibits a maximum absorbance of 646 nm in the visible region, similar to the value of 648 nm reported for a six-coordinate Cu^{II} cyclen complex bearing a picolinate pendant group [33]. Similarly, the complexes bearing the tetradentate ligands **2-4** show absorption bands in the range 603-621 nm (Figure S13), indicative of five-coordinate Cu^{II} species [33].

To confirm that the Cu^{2+} ions responsible for $A\beta_{40}$ aggregation were subsequently chelated upon introduction of the cyclen compounds **1-4**, and that unbound $A\beta_{40}$ was returned to solution, aliquots of the supernatant from centrifuged $A\beta_{40}/Cu^{2+}/cyclen$ mixtures were examined using ESI-MS (Table 2 and ESI). The data obtained from $A\beta_{40}/Cu^{2+}$ samples prior to treatment with **1-4** contained no signal for $A\beta_{40}$ indicating that the aggregates were insoluble. The treated samples contained signals for $A\beta_{40}$ species with different degrees of protonation as well as the corresponding cyclen-Cu complex. Thus, the de-aggregation of the insoluble $A\beta_{40}$ can be ascribed to the chelators' ability to irreversibly sequester the aggregate-inducing Cu^{2+} ions.

The antioxidant activities of **1**-**4** were evaluated using the 1,1-diphenyl-2-picrylhydrazyl (DPPH) scavenging assay [34] using ascorbic acid as a reference material. DPPH is a stable free radical that can be scavenged by efficient antioxidants. Thus, the decrease in optical absorbance (at a wavelength corresponding to that of DPPH absorbance) upon introduction of an antioxidant provides a measure of the free radical scavenging activity.
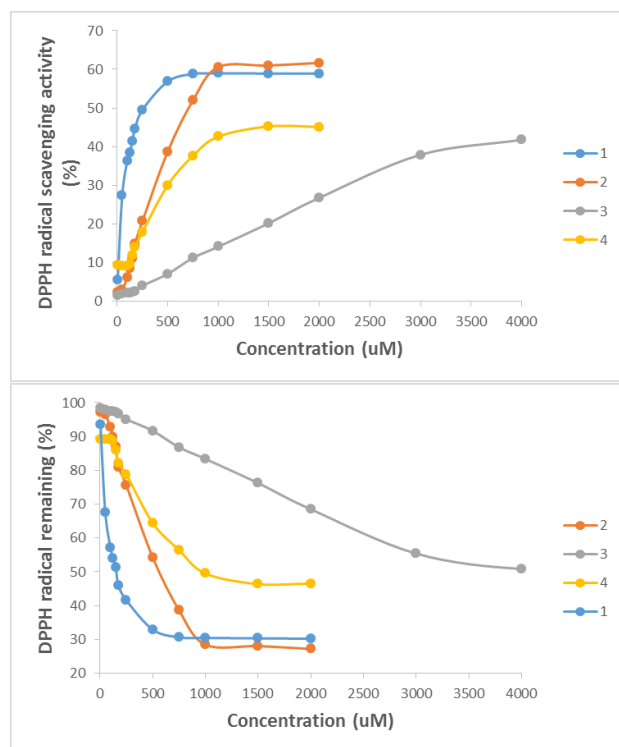

Fig. 5: (Top) graph showing the scavenging activity of the DPPH radical by cyclen compounds and (bottom) the percentage of DPPH radicals remaining in solution after the reactions with **1**-**4**.

Fig. 5 shows the measured radical scavenging activities (above panel), and the percentages of DPPH radical remaining after reaction (below panel) for **1**-**4** while IC_{50} data are presented in Table 3. All of the tested compounds exhibit activities lower than that of ascorbic acid. Compound **3** shows a very low activity ($IC_{50} > 500$ μM) whereas **1** has a reasonable activity with an IC_{50} value of 71 μM. Compounds **2** and **4** have modest antioxidant properties (IC50 ~400 μM).

Table 3: IC_{50} data from DPPH assays.

Compound	IC_{50} (µM)
Vit. C	22 ± 3
1	71 ± 4
2	400 ± 14
3	1630 ± 21
4	440 ± 12

Pharmacokinetic properties of **1**-**4** were calculated and the data are collected in Table S10. Compounds **1**-**3** have predicted physicochemical properties that would provide adequate blood-brain barrier (BBB) permeability, while **4** is predicted not to penetrate the BBB to any significant degree. Each compound is predicted to be a non-inhibitor for CYP2D6 and well-metabolized in the first phase metabolism. All of the compounds have polar surface area (PSA) < 140 $Å^2$ and AlogP98 (logarithm of the partition coefficient between n-octanol and water at the 98% confidence level) <5 with the exception of **4**. A plot of these two parameters (Figure S12) shows that **1, 2** and **3** are highly likely to have adequate intestinal absorption and BBB permeability while **4** is less likely to possess to do so.

Conclusions

Compounds based on the cyclen macrocycle that bear pendant groups have been synthesized and characterized. Each of the compounds **1-4** has been shown to coordinate Cu^{2+}, Zn^{2+} and Ni^{2+} metal ions in aqueous solution. X-ray crystal structures revealed that **1** binds in a hexadentate fashion while **2** and **3** are tetradentate. Importantly, each of the compounds can remove Cu^{2+} ions from A β_{40} to inhibit aggregation. Of the four chelating compounds, **1** was superior in returning aggregated $A\beta_{40}$ to solution compared to **2-4**. In terms of anti-oxidant properties, **1** showed the greatest free radical scavenging activity although none were greater than Vitamin C.

Experimental Section

General: Reagents and analytical grade solvents were purchased from commercial sources. The $A\beta_{40}$ peptide (purity >95%) was purchased from GL Biochem Ltd (Shanghai). Anhydrous dichloromethane, triethylamine and acetonitrile were prepared by refluxing over calcium hydride for several hours. Anhydrous toluene was prepared by standing over sodium wire for 2 days. 1,4,7,10-tetrazacyclododecane was synthesized according to the procedure of Reed and Weisman [35]. Pierce BCA protein assay kit was obtained from Thermo Scientific.

^{1}H and ^{13}C NMR spectra were recorded on an Agilent 500 MHz spectrometer (500 MHz ^{1}H, 125 MHz ^{13}C) using deuterated chloroform (CDCl$_3$) as solvent unless otherwise specified. Low-resolution mass spectra were obtained on an Agilent 6890GC fitted with 5% polysilphenylene, 95% polydimethylsiloxane column, and an Agilent 5973n MS (EI) spectrometer. High-resolution mass spectra were obtained on an Agilent 6510 Accurate Mass Q-TOF Mass Spectrometer, equipped with an ESI source. TLC analysis was performed using aluminium-backed Merck 60 GF$_{254}$ silica gel or Merck 60 GF$_{254}$ neutral alumina gel with UV detection at 254 nm. Compounds were purified by column chromatography using either neutral alumina or silica gel (40 – 63 μm).

Suitable single crystals were selected for crystallographic studies using a polarizing microscope (Leica M165Z), mounted on a MicroMount (MiTeGen, USA) consisting of a thin polymer tip with a wicking aperture. The X-ray diffraction measurements were carried out on a Bruker kappa-II CCD diffractometer at 150 K by using IμS Incoatec Microfocus Source with Mo-Kα radiation (λ = 0.710723 Å) . The single crystal, mounted on the goniometer using cryo loops for intensity measurements, was coated with paraffin oil and then quickly transferred to the cold stream using an Oxford Cryo stream attachment. Symmetry related absorption corrections using the program SADABS[36] were applied and the data were corrected for Lorentz and polarisation effects using Bruker APEX2 software[37]. The

structure was solved by Direct methods and the full-matrix least-square refinement was carried out using Shelxl[38] in Olex2[39]. The non-hydrogen atoms were refined anisotropically. The molecular graphic was generated using program Olex2 [39].

Pharmacokinetics parameters were calculated using Discovery Studio 4.5 (Accelrys, San Diego, CA, USA).

Synthesis: *Synthesis of 2-bromomethyl-8-hydroxyquinoline:* 2-Formyl-8-hydroxyquinoline (2.0 g, 0.010 mol) was dissolved in methanol (25 mL) in a 50 mL round bottom flask. Sodium borohydride (0.50 g, 0.013 mol) was added gradually and the reaction stirred for 5 hours at room temperature. The solvent was removed using a rotary evaporator and then water (25 mL) was added. The resultant solution was neutralized using aqueous hydrochloric acid (2 M) and then extracted with ethyl acetate (3 x 50 mL) and the organic phase dried over sodium sulfate. The mixture was filtered and the solvent was evaporated by rotary evaporator to yield 2-hydroxymethyl-8-hydroxyquinoline (1.66 g, 95%), which was used without further purification. 2-Hydroxymethyl-8-hydroxyquinoline (1.66 g, 9.5 mmol) was added to a 25 ml round bottom flask and concentrated hydrobromic acid (16 mL) was added dropwise. The mixture was stirred at reflux for 4 hours and then cooled in an ice bath. Aqueous sodium carbonate (2 M) was added until pH 7. The mixture was extracted with dichloromethane (3 x 50 mL) and the organic layer was dried over sodium sulfate, filtered, and the solvent was evaporated using a rotary evaporator. The crude product was purified by silica gel column chromatography eluting with hexane: ethyl acetate (1:1) to give pure 2-bromomethyl-8-hydroxyquinoline as a pale yellow solid (1.4 g, 82 %). Note: This compound was found to decompose upon standing in air after 2 days. RF silica gel (hexane: ethyl acetate (1:1)) = 0.921; ^{1}H NMR (δ, 500 MHz, CDCl$_3$) 4.71 (s, 2H), 7.20 (d, J=8 Hz, 1H), 7.34 (d, J= 8 Hz, 1H), 7.47 (td, J1= 8.5 Hz, J2=2 Hz, 1H), 7.58 (dd, J1= 8.5 Hz, J2= 1.5 Hz, 1H), 8.06 (s, 1H), 8.18 (dd, J1= 8.5 Hz, J2= 1.5 Hz, 1H). ^{13}C NMR (δ, 125.7 MHz, CDCl$_3$) 33.9, 110.8,

117.8, 122.0, 127.8, 128.5, 137.6, 152.2, 154.9; HRMS [M+H]$^+$ calc. $C_{10}H_8ONBr$ 237.9862, Found 237.9868.

Synthesis of 2-bromo-N-(2-(pyridin-2-yl)ethyl) acetamide: 2-(pyridin-2-yl)ethan-1-amine (2.44 ml, 20 mmol) and triethylamine (2.78 mL, 20 mmol) were dissolved in anhydrous dichloromethane (25ml) and then cooled to -10°C. A solution of bromoacetyl bromide (1.74 ml, 20 mmol) in anhydrous dichloromethane (10 ml) was added dropwise. The mixture was stirred for 1 h under a nitrogen atmosphere at -10 °C and then for 2 hours at room temperature. The reaction mixture was extracted with aqueous sodium bicarbonate and the aqueous phase extracted with dichloromethane (3 x 50 mL). The combined organic extracts were dried with anhydrous potassium carbonate the solvent was removed using a rotary evaporator to give a pale yellow oil (3.93 g, 81%). ^{1}H NMR (δ, 500 MHz, CDCl$_3$) 3.02 (t, J= 6Hz, 2H), 3.71 (q, J=6 Hz, 2H), 3.86 (s, 2H), 7.17 (m, 2H), 7.63 (td, J1= 7.5 Hz, J2=2 Hz, 1H), 7.67 (s, 1H), 8.55 (dd, J1= 5.5 Hz, J2= 1.5 Hz, 1H) ppm; ^{13}C NMR (δ, 125.7 MHz, CDCl$_3$) 29.5, 36.4, 39.4, 121.9, 123.6, 136.9, 149.4, 159.4, 166.0 ppm; HRMS [M]$^+$ calculated for $C_9H_{11}N_2OBr$ 242.0055 Found 242.0063.

Synthesis of bis(2-hydroxyethyl)carbamic bromide: Using the procedure described above and using diethanolamine (1.92 mL, 20 mL) instead of 2-(pyridin-2-yl)ethan-1-amine, a yellow oil (4.07 g, 90%) was obtained; ^{1}H NMR (δ, 500 MHz, CDCl$_3$) 3.54 (m, 4H), 3.83 (m, 4H), 4.04 (s, 2H) ppm; ^{13}C NMR (δ, 125.7 MHz, CDCl$_3$) 26.4, 49.5, 59.9, 169.4; HRMS [M+H]$^+$ calculated for $C_6H_{12}NO_3Br$ 226.0073 Found 226.0079.

*Typical procedure for the synthesis of **1-4** - Synthesis of N-(2-methyl-8-hydroxyquinoline)-1,4,7,10-tetrazacyclododecane (**1**):* 1,4,7,10-tetrazacyclododecane (0.288 g, 1.68 mmol) was dissolved in anhydrous acetonitrile (20 ml) in a two-necked round bottom flask (50 ml) containing potassium carbonate (0.58 g, 4.2 mmol)). Separately, 2-bromomethyl-8-hydroxyquinoline (0.2 g, 0.84 mmol, a cyclen:alkylbromide ratio of 2:1) was dissolved in

anhydrous acetonitrile (10ml) and was added dropwise to the 1,4,7,10-tetrazacyclododecane solution over 2 hours under a flush of nitrogen gas and at reflux. After 48 hours the mixture was cooled and filtered. The crude product was purified by column chromatography (silica gel) eluting with dichloromethane: methanol: ammonia (83:15:2). Compound **1** was obtained as a dark yellow oil (0.165 g, 60 %). RF silica gel (dichloromethane: methanol: ammonia 83:15:2) = 0.56. ^{1}H NMR (δ, 500 MHz, CDCl$_3$) 2.78-2.92 (m, 16H), 4.02 (s, 2H), 7.14 (d, J=7 Hz, 1H), 7.21 (d, J= 8 Hz, 1H), 7.28 (d, J= 9 Hz, 1H), 7.32 (t, J= 8 Hz, 1H), 8.02 (d, J= 9 Hz, 1H) ppm. ^{13}C NMR (δ, 125.7 MHz, CDCl$_3$) 45.4, 45.9, 46.3, 46.8, 52.6, 111.5, 116.8, 120.5, 126.6, 127.4, 136.1, 151.7, 159.9 ppm; HRMS [M+H]$^+$ calculated for C$_{18}$H$_{27}$ON$_5$ 330.2288 Found 330.2291; FTIR (neat) 3393, 3350, 3005, 2918, 1653, 1558, 1458, 1458, 1296, 1063, 815.cm^{-1}.

*Synthesis of N-[2-(pyridin-2-yl)ethyl] acetamide-1,4,7,10-tetrazacyclododecane (**2**):* Using 2-bromo-*N*-(2-(pyridin-2-yl)ethyl) acetamide as the pendent arm group, the crude product was purified by column chromatography (alumina) eluting with chloroform: methanol: 3:1. Compound **2** was isolated as a brown oil (65%). RF alumina (chloroform: methanol 3:1) = 0.26; ^{1}H NMR (δ, 500 MHz, CDCl$_3$) 2.57-2.77 (m, 16H), 3.04 (t, J= 8.5 Hz, 2H), 3.12 (s, 2H), 3.68 (q, J=6.5 Hz, 2H), 7.13 (t, 1H, J= 7.5 Hz), 7.21 (d, 1H, J= 7.5 Hz), 7.61 (td, J1= 7.5 Hz, J2= 1.5 Hz, 1H), 8.14 (s, 1H), 8.53 (dd, J1= 5.5 Hz, J2= 1 Hz, 1H) ppm. ^{13}C NMR (δ, 125.7 MHz, CDCl$_3$) 29.8, 37.6, 45.9, 46.9, 47.4, 53.3, 59.5, 121.6, 123.6, 136.7, 149.3, 159.9, 171.8 ppm. HRMS [M+H]$^+$ calculated for C$_{17}$H$_{30}$N$_6$O 335.2554 Found 335.2558; FTIR (neat) 3418, 3180, 3078, 2920, 1669, 1632, 1595, 1473, 1437, 1358, 771 cm^{-1}.

*Synthesis of N-[3-(pyridin-4-yl)propyl]-1,4,7,10-tetrazacyclododecane (**3**):* Using 4-(3-bromopropyl)pyridine as the pendent arm group, the crude product was purified by silica gel column chromatography eluting with dichloromethane: methanol: ammonia 82:15:2 compound **3** with white solid (62%). RF silica gel 0.26; ^{1}H NMR (δ, 500 MHz, CDCl$_3$) 1.80

(m, 2H), 2.46 (t, J=7.5 Hz, 2H), δ = 2.54-2.63 (m, 16H), 2.78 (t, J=5 Hz, 2H), 7.14 (d, 2H, J=6Hz, 2H), 8.45 (d, J= 6 Hz, 2H) ppm; ^{13}C NMR (δ, 125.7 MHz, CDCl$_3$): 28.1, 33.1, 44.9, 45.8, 46.8, 51.5 , 54.0, 123.9, 149.6, 151.4 ppm; HRMS [M+H]$^+$ calculated for C$_{16}$H$_{29}$N$_5$ 292.2496 Found 292.2506; FTIR (neat) 3417, 2920, 2850, 1659, 1604, 1453, 1261, 801 cm^{-1}.

Synthesis of N-(bis(2-hydroxyethyl)carbamic bromide)-1,4,7,10-tetrazacyclododecane (4): Using bis(2-hydroxyethyl)carbamic bromide as the pendent arm, the crude product was washed with hot hexane and then with hot toluene to give an orange oil (61%). ^{1}H NMR (δ, 500 MHz, CDCl$_3$) δ = 2.57-2.78 (m, 16H), 3.41 (s, 2H), 3.46 (t, J= 4.5 Hz, 2H), 3.66 (t, J= 5 Hz, 2H), 3.70 (m, 4H) ppm; ^{13}C NMR (δ, 125.7 MHz, CDCl$_3$): 44.5, 45.0, 45.7, 46.2, 49.3, 49.7, 52.4, 59.1, 59.4, 171.9 ppm; HRMS [M+H]$^+$ calculated for C$_{14}$H$_{31}$N$_5$O$_3$ 318.2499 Found 318.2516; FTIR (neat) 3377, 3250, 2934, 1635, 1559, 1457, 1292, 1071 cm^{-1}.

Typical procedure for the synthesis of Zn and Ni complexes of 1-4 - Synthesis of Zn-1: N-(2-methyl-8-hydroxyquinoline)-1,4,7,10-tetrazacyclododecane (**1**, 30 mg, 0.0911mmol) was dissolved in methanol (~1 mL) and ZnCl$_2$ (12.42 mg, 0.0911 mmol) was dissolved in water (~1 mL). The metal salt solution was added dropwise to the methanolic solution. Crystals suitable for X-ray diffraction were grown by diffusion of acetone into the methanol/water solution in a sealed vessel. Yield of green solid (80 %). ^{1}H NMR (δ, 500 MHz, D$_2$O) 2.87-3.24 (m, 16H), 4.40 (s, 2H), 7.33 (dd, J1=8 Hz, J2=2 Hz, 1H), 7.42 (t, J= 8.5 Hz, 1H), 7.59 (m, 2H), 8.52 (d, J= 8.5 Hz, 1H) ppm; ^{13}C NMR (δ, 125.7 MHz, D$_2$O): = 46.5, 46.8, 47.0, 56.0, 60.9, 115.8, 121.3, 123.4, 130.3, 131.0, 131.2, 143.3, 160.0 ppm; HRMS [M]$^+$/2 calculated for ZnC$_{18}$H$_{27}$ON$_5$ 196.5748 Found 196.5748 with % abund. m/z 196.5748 (100), 197.0766 (21.62), 197.5737 (60.1), 198.0747 (21.23), 198.5731 (42.59), 199.0732 (8.81); FTIR (neat) 3416, 3215, 2930, 1621, 1560, 1456, 1476, 1384, 1144, 756 cm^{-1}; UV (MeOH, ε(M^{-1}, cm^{-1})) λ 252(14218), 205(13270)

Synthesis of Zn-2: Yellow solid (82%). ^{1}H NMR (δ, 500 MHz, D$_2$O) 2.65-2.97 (m, 16H), δ = 3.04 (m, 2H), 3.43 (s, 2H), 3.69 (t, J= 6.5 Hz, 2H), 7.39 (m, 2H), 7.88 (td, J1= 7.5 Hz, J2= 2 Hz, 1H), 8.48 (d, J= 4.5 Hz, 1H), ppm; ^{13}C NMR, δ = 38.6, 42.1, 46.9, 47.3, 48.7, 56.7, 58.3, 125.2, 127.2, 141.4, 150.5, 160.4, 175.1 ppm; HRMS [M]$^+$/2 calculated for ZnC$_{17}$H$_{30}$N$_6$O 199.0881 Found 199.0890 with % abund. m/z 199.089 (100), 199.5899 (20.96), 200.0874 (60.24), 200.5881 (20.83), 201.0868 (42.54), 201.588(8.54), 202.0877(2.23); FTIR (neat) 3469, 3285, 3081 , 2930 1657, 1641, 1593, 1476, 1442, 1384, 772 cm^{-1}; UV (MeOH, ε(M^{-1}, cm^{-1})) λ 261.5(12727), 208(14182).

Synthesis of Zn-3: White solid (75%). ^{1}H NMR (D$_2$O), δ: 1.950 (m, 2H), 2.71 (t, J=7Hz, 2H), 2.92-2.99 (m, 16H), 3.05(m, 2H), 7.54 (d, 2H, J=6Hz), 8.44 (d, J= 6 Hz, 2H) ppm; ^{13}C NMR δ: 25.2, 34.7, 44.9, 46.0 47.0, 52.2, 54.71, 127.6, 150.6, 151.2 ppm; HRMS [M]$^+$ /2 calculated for ZnC$_{16}$H$_{29}$N$_5$ 177.5852 Found 177.5723 with % abund. m/z 177.5723(100), 178.0871(19.47) 178.5842 (59.76), 179.0854 (19.88), 179.5843 (42.12); FTIR (neat) 3465, 2937, 2933, 1658, 1605, 1443 1296, 810 cm^{-1}, UV (MeOH, ε(M^{-1}, cm^{-1})) λ 255(5360), 207(11504).

Synthesis of Zn-4: Yellow solid (81%). ^{1}H NMR (D$_2$O) δ = 2.78-3.11 (m, 16H), 3.57 (t, J= 5.5 Hz, 2H), 3.67 (t, J= 5.5 Hz, 2H), 3.80 (t, J= 5.5Hz, 4H), 3.87 (s, 2H) ppm; ^{13}C NMR δ: 46.4, 47.7, 49.1, 50.7, 51.5, 58.3, 58.7, 60.6, 61.0, 176.7 ppm; HRMS [M]$^+$/2 calculated for ZnC$_{14}$H$_{31}$N$_5$O$_3$ 190.5854 Found 190.5890 with % abund. m/z 190.5890(100), 191.091(17.44) 191.5875 (60.02), 192.0884 (18.77), 192.5869 (42.12); FTIR (neat) 3421, 3261, 2932, 1616, 1559, 1457, 1297, 1091 cm^{-1}; UV (MeOH, ε(M^{-1}, cm^{-1})) λ 204(7173)

Synthesis of Ni-1: Using NiSO$_4$·7H2O, a yellow solid was obtained (78 %). HRMS [M]$^+$/2 calculated for NiC$_{18}$H$_{27}$ON$_5$ 193.5779 Found 193.5784 with % abund. m/z 193.5784 (100), 194.0797 (21.64), 194.5763 (40.92), 195.1595 (10.2), 195.5753 (6.67); FTIR (neat) 3249,

3220, 2920, 1653, 1653, 1457, 1384, 1150, 794 cm^{-1}; UV (MeOH, ε(M^{-1}, cm^{-1})) λ 260(4800), 244(4533), 202(6533)

Synthesis of Ni-2: Using NiSO$_4$·7H2O, a white solid was obtained (71%). HRMS [M]$^+$/2 calculated for NiC$_{17}$H$_{30}$N$_6$O 196.0912 Found 196.0919 with % abund. m/z 196.0919 (100), 196.5932 (20.96), 197.0898 (40.83), 197.5908 (9.93), 198.0890 (6.58), 198.5901(1.22), 199.0891(1.48); FTIR (neat) 3423, 3285, 2941, 1637, 1642, 1596, 1472, 1389, 777 cm^{-1}; UV (MeOH, ε(M^{-1}, cm^{-1})) λ 262(4545), 207(13182).

Synthesis of Ni-3: Using NiSO$_4$·7H2O, a bright blue solid was obtained (86%). HRMS [M]$^+$/2 calculated for NiC$_{16}$H$_{29}$N$_5$ 174.5883 Found 174.5823 with % abund. m/z 174.5823(100), 175.0866(19.47) 175.5821 (40.32), 176.0854 (9.28), 176.5823 (6.36); FTIR (neat) 3466, 2942, 2928, 1651, 1601, 1438, 1292, 812 cm^{-1}; UV (MeOH, ε(M^{-1}, cm^{-1})) λ 254(4000), 207(12000).

Synthesis of Ni-4: Using NiSO$_4$·7H2O a green solid was obtained (85%). HRMS [M]$^+$/2 calculated for NiC$_{14}$H$_{31}$N$_5$O$_3$ 187.5885 Found 187.5884 with % abund. m/z 187.5884(100), 188.0898(17.45) 188.5866 (40.58), 189.0872 (8.56), 189.5852 (6.42); FTIR (neat) 3258, 1616, 1457, 1098 cm^{-1}; UV (MeOH, ε(M^{-1}, cm^{-1})) λ 206(12760)

Typical procedure for the synthesis of Cu complexes of 1-4 - Synthesis of Cu-1: N-(2-methyl-8-hydroxyquinoline)-1,4,7,10-tetrazacyclododecane (**1,** 30mg, 0.0911mmol) was dissolved in methanol (~1 mL) and separately CuSO$_4$.5H$_2$O (22.75 mg, 0.0911 mmol) was dissolved in methanol (~1 mL). The copper(II) sulfate solution was added to the solution containing the chelator dropwise. Crystals suitable for X-ray diffraction were grown by diffusion of diethyl ether into the methanolic solution in a sealed vessel. Yield of green solid (82 %). HRMS [M]$^+$/2 calculated for CuC$_{18}$H$_{27}$ON$_5$ 196.0756 Found 196.0755 with % abund. m/z 196.0755 (100), 196.5766 (21.62), 197.0748 (47.05), 197.5758 (9.83); FTIR (neat) 3446,

3211, 2928, 1653, 1559, 1457, 1476, 1384, 1117, 812 cm^{-1}; UV (MeOH, ε(M^{-1}, cm^{-1})) λ 646(143), 253(8333), 204(8095)

Synthesis of Cu-2: Blue solid (75%). HRMS [M]$^+$/2 calculated for CuC$_{17}$H$_{30}$N$_6$O 198.5883 Found 198.5899 with % abund. m/z 198.5899 (100), 199.0903 (20.96), 199.5884(46.92), 200.0894 (9.52), 200.5905 (1.06); FTIR (neat) 3442 & 3260, 3083, 2941, 1640, 1595, 1477, 1443, 1384, 771 cm^{-1}; UV (MeOH, ε(M^{-1}, cm^{-1})) λ 616(97), 262(6818), 207(8727).

Synthesis of Cu-3: Blue solid (91%). HRMS [M]$^+$/2 calculated for CuC$_{16}$H$_{29}$N$_5$ 177.0854 Found 177.0858 with % abund. m/z 177.0858(100), 177.5872(19.47) 178.085 (46.41), 178.5863 (8.79); FTIR (neat) 3408, 2935, 2936, 1658, 1612, 1448, 1292, 812 cm^{-1}; UV (MeOH, ε(M^{-1}, cm^{-1})) λ 621(186), 257(3200), 204(4000)

Synthesis of Cu-4: Blue solid (26.2472 mg, 0.0688 mmol). Yield 77%; HRMS [M]$^+$/2 calculated for CuC$_{14}$H$_{31}$N$_5$O$_3$ 190.0856 Found 190.0876 with % abund. m/z 190.0876(100), 190.5885(17.44) 191.0868 (46.66), 191.5878 (7.94); FTIR (neat) 3224, 2933, 1611, 1457, 1291, 1116 cm^{-1}; UV (MeOH, ε(M^{-1}, cm^{-1})) λ 603(194), 272(3670), 200(10229)

Antioxidant activity measured by DPPH assay: The 1,1-diphenyl-2-picrylhydrazyl (DPPH) assay was used to measure antioxidant activity This assay was performed according a modified published method [34]. In brief, stock solutions (10 mM in methanol) of **1-4** and a 200 μM methanolic DPPH solution were prepared. A stock solution of ascorbic acid (1 mM in methanol) was used as a control. DPPH (200μM, 50μl) was added to 150μl of sample solutions (ascorbic acid, **1-4**) with different concentrations using 96 well microplates. Each of the additions was performed in triplicate. The microplates were wrapped in aluminum foil and kept at 30 °C for 30 minutes in the dark. Spectrophotometric measurements were recorded using a Thermolabsystems Multiskan Ascent spectrophotometer at 520 nm.

Measurements were performed ensuring no exposure to ambient light. Activities were calculated as follows:

DPPH radical scavenging activity (%) = [(Abs$_{control}$ − Abs$_{compound}$)]/(Abs$_{control}$)] × 100

where Abs$_{control}$ is the absorption of (200μM, 50μL) DPPH with 150μL of neat methanol and Abs$_{compound}$ is the absorption of test compounds at different concentrations plus DPPH (200μM, 50μL). The percentage of remaining DPPH radical is calculated using:

DPPH remaining in the reaction (%) = [(Abs$_{compound}$ − Abs$_{blank}$)/(Abs$_{control}$ − Abs$_{blank}$)] × 100

where Abs$_{blank}$ is the absorption of pure methanol. The IC$_{50}$ ascorbic acid (vitamin C) and **1-4** is the samples concentration at which 50% of the DPPH free radical was scavenged.

Assays to assess interactions with Aβ$_{40}$

Turbidity assay: This assay was used to assess the Cu^{2+}-induced aggregation and was performed according a modified published method [30]. Briefly, aqueous copper(II) sulfate (4 μL, 5 mM) and buffer solution (10 μL, Tris-HCl (200 mM) / NaCl (1.5 M), pH 7.4) were added to aqueous Aβ$_{40}$ (50 μL, 170 μM). The solution was incubated at 37 ºC for 48 hours to prepare the aggregated Cu(II)/Aβ$_{40}$ sample. Then, **1-4** (10 μL, 4mM,) were added individually followed by incubation at 37 ºC for 4 hours. Buffer solution (600 μL, Tris-HCl (20 mM), NaCl (150 mM) pH 7.4) was added to dilute the samples. Buffer solution (624 μL and 610 μL, Tris-HCl (20 mM), NaCl (150 mM) pH 7.4) was added to Aβ$_{40}$ and Cu(II)/Aβ$_{40}$ samples, respectively. For each sample, 200 μL was added to a 96 well microplate and performed in triplicate. The UV-visible absorbance was measured at 405 nm.

*Concentrations of Aβ$_{40}$ measured before and after de-aggregation with **1-4** :* Six 500 μL vials were labeled as Aβ$_{40}$, Cu(II)/Aβ$_{40}$ and Cu(II)/Aβ$_{40}$/**1** (or **2, 3, 4**). Aqueous Aβ$_{40}$ (50 μL,

170 μM) and buffer solution (50 μL, Tris-HCl (200 mM) / NaCl (1.5 M), pH 7.4) were added to the Aβ40 vial. Aqueous copper (II) sulfate (4 μL, 5 mM), buffer solution (46 μL, Tris-HCl (200 mM) / NaCl (1.5 M), pH 7.4) and aqueous Aβ40 (50 μL, 170 μM) were added to the Cu (II)/Aβ40 vial. Cu (II)/Aβ40/**1-4** vials were prepared using the same method as for the Cu (II)/Aβ40 vial except 36 μL of buffer solution was added. The resultant solutions were incubated at 37 °C for 48 hours. After 48 hrs, **1-4** (10 μL, 4mM) were added to the Cu(II)/Aβ40/**1-4** vials followed by incubation at 37 °C for 4 hours.

To a 96 well microplate, we added 25 μL from each vial plus 200 μL of prepared BCA assay reagents. On the same plate, 25 μL of different concentrations of bovine serum albumin plus 200 μL of the reagents were added. Each of the additions was performed in triplicate. The colour change monitored by UV-visible absorbance using a microplate reader at 540 nm.

Mass spectrometric analysis of chelated species: Samples prepared using the procedure outlined in 4.4.1 (before the addition of **1-4**) were centrifuged (12000 rpm) for 30 minutes to precipitate any undissolved material. The supernatant was decanted, the pellet was washed with water, centrifuged a second time (12000 rpm) for 30 minutes, and the supernatant decanted. Aqueous solutions of **1-4** (5 μL, 4mM) were added followed by incubation at 37 °C for 4 hours. The pH was adjusted at 7.4 (aq. NaOH (0.5M) or aq. HCl (0.5 M)) and the mixture was centrifuged (12000 rpm) for 30 minutes. Aliquots of the supernatant were examined using ESI-MS.

Acknowledgments

Supplementary Data

CCDC1510634, CCDC 1510645, CCDC 1510646, CCDC 1510652 contains supplementary crystallographic data for Zn-**1**, Cu-**2**, Cu-**3** and Ni-**3** respectively. Supplementary data contains selected crystallographic data, mass spectrometric data and DPPH scavenging activities.

References

[1] M. Goedert, M.G. Spillantini, A century of alzheimer's disease, Science, 314 (2006) 777-781.

[2] Z. Chen, C. Zhong, Oxidative stress in alzheimer's disease, Neurosci Bull, 30 (2014) 271-281.

[3] P. Faller, Copper and zinc binding to amyloid-beta: Coordination, dynamics, aggregation, reactivity and metal-ion transfer, Chembiochem, 10 (2009) 2837-2845.

[4] N.E. Wezynfeld, E. Stefaniak, K. Stachucy, A. Drozd, D. Płonka, S.C. Drew, A. Krężel, W. Bal, Resistance of cu (aβ4–16) to copper capture by metallothionein-3 supports a function for the aβ4–42 peptide as a synaptic cuii scavenger, Angewandte Chemie International Edition, 55 (2016) 8235-8238.

[5] N.T. Watt, I.J. Whitehouse, N.M. Hooper, The role of zinc in alzheimer's disease, International Journal of Alzheimer's Disease, 2011 (2010).

[6] K. Wild, A. August, C.U. Pietrzik, S. Kins, Structure and synaptic function of metal binding to the amyloid precursor protein and its proteolytic fragments, Frontiers in Molecular Neuroscience, 10 (2017).

[7] A.I. Bush, W. Pettingell, M. De Paradis, R.E. Tanzi, W. Wasco, The amyloid beta-protein precursor and its mammalian homologues. Evidence for a zinc-modulated heparin-binding superfamily, Journal of Biological Chemistry, 269 (1994) 26618-26621.

[8] V.W. Chow, M.P. Mattson, P.C. Wong, M. Gleichmann, An overview of app processing enzymes and products, Neuromolecular medicine, 12 (2010) 1-12.

[9] C. Becker-Pauly, C.U. Pietrzik, The metalloprotease meprin β is an alternative β-secretase of app, Frontiers in Molecular Neuroscience, 9 (2017) 159.

[10] I. Singh, A.P. Sagare, M. Coma, D. Perlmutter, R. Gelein, R.D. Bell, R.J. Deane, E. Zhong, M. Parisi, J. Ciszewski, Low levels of copper disrupt brain amyloid-β homeostasis by altering its production and clearance, Proceedings of the National Academy of Sciences, 110 (2013) 14771-14776.

[11] G.J. Brewer, Issues raised involving the copper hypotheses in the causation of alzheimer's disease, International Journal of Alzheimer's Disease, 2011 (2011).

[12] L. Guilloreau, S. Combalbert, A. Sournia-Saquet, H. Mazarguil, P. Faller, Redox chemistry of copper–amyloid-β: The generation of hydroxyl radical in the presence of ascorbate is linked to redox-potentials and aggregation state, ChemBioChem, 8 (2007) 1317-1325.

[13] G.P. Morris, I.A. Clark, B. Vissel, Inconsistencies and controversies surrounding the amyloid hypothesis of alzheimer's disease, Acta Neuropathologica Communications 2(2014) 135-156.

[14] I. Naletova, V.G. Nicoletti, D. Milardi, A. Pietropaolo, G. Grasso, Copper, differently from zinc, affects the conformation, oligomerization state and activity of bradykinin, Metallomics, 8 (2016) 750-761.

[15] R. Leon, A.G. Garcia, J. Marco-Contelles, Recent advances in the multitarget-directed ligands approach for the treatment of alzheimer's disease, Med Res Rev, 33 (2013) 139-189.

[16] R.A. Cherny, C.S. Atwood, M.E. Xilinas, D.N. Gray, W.D. Jones, C.A. McLean, K.J. Barnham, I. Volitakis, F.W. Fraser, Y.-S. Kim, Treatment with a copper-zinc chelator markedly and rapidly inhibits β-amyloid accumulation in alzheimer's disease transgenic mice, Neuron, 30 (2001) 665-676.

[17] A.S. Pithadia, M.H. Lim, Metal-associated amyloid-beta species in alzheimer's disease, Curr Opin Chem Biol, 16 (2012) 67-73.

[18] R.Y. Alta, H.A. Vitorino, D. Goswami, C.W. Liria, S.P. Wisnovsky, S.O. Kelley, M.T. Machini, B.P. Espósito, Mitochondria-penetrating peptides conjugated to desferrioxamine as chelators for mitochondrial labile iron, PloS one, 12 (2017) e0171729.

[19] D.G. Smith, R. Cappai, K.J. Barnham, The redox chemistry of the alzheimer's disease amyloid β peptide, Biochimica et Biophysica Acta (BBA)-Biomembranes, 1768 (2007) 1976-1990.

[20] V. Moret, Y. Laras, N. Pietrancosta, C. Garino, G. Quéléver, A. Rolland, B. Mallet, J.-C. Norreel, J.-L. Kraus, 1, 1′-xylyl bis-1, 4, 8, 11-tetraaza cyclotetradecane: A new potential copper chelator agent for neuroprotection in alzheimer's disease. Its comparative effects with clioquinol on rat brain copper distribution, Bioorganic & medicinal chemistry letters, 16 (2006) 3298-3301.

[21] D. Rogolino, A. Cavazzoni, A. Gatti, M. Tegoni, G. Pelosi, V. Verdolino, C. Fumarola, D. Cretella, P.G. Petronini, M. Carcelli, Anti-proliferative effects of copper (ii) complexes with hydroxyquinoline-thiosemicarbazone ligands, European Journal of Medicinal Chemistry, 128 (2017) 140-153.

[22] C. Rodríguez-Rodríguez, M. Telpoukhovskaia, C. Orvig, The art of building multifunctional metal-binding agents from basic molecular scaffolds for the potential application in neurodegenerative diseases, Coordination Chemistry Reviews, 256 (2012) 2308-2332.

[23] R. Delgado, V. Felix, L.M.P. Lima, D.W. Price, Metal complexes of cyclen and cyclam derivatives useful for medical applications: A discussion based on thermodynamic stability constants and structural data, Dalton Transactions, DOI 10.1039/B704360K(2007) 2734-2745.

[24] X. Liang, P.J. Sadler, Cyclam complexes and their applications in medicine, Chemical Society Reviews, 33 (2004) 246-266.

[25] A.F. Martins, A.C. Oliveira, J.-F. Morfin, D.V. Laurents, É. Tóth, C.F. Geraldes, Associating a negatively charged gddota-derivative to the pittsburgh compound b for targeting aβ amyloid aggregates, JBIC Journal of Biological Inorganic Chemistry, 21 (2016) 83-99.

[26] M.-A. Yoon, T.-S. Jeong, D.-S. Park, M.-Z. Xu, H.-W. Oh, K.-B. Song, W.S. Lee, H.-Y. Park, Antioxidant effects of quinoline alkaloids and 2, 4-di-tert-butylphenol isolated from scolopendra subspinipes, Biological and Pharmaceutical Bulletin, 29 (2006) 735-739.

[27] L. Lannfelt, K. Blennow, H. Zetterberg, S. Batsman, D. Ames, J. Harrison, C.L. Masters, S. Targum, A.I. Bush, R. Murdoch, Safety, efficacy, and biomarker findings of pbt2 in targeting aβ as a modifying therapy for alzheimer's disease: A phase iia, double-blind, randomised, placebo-controlled trial, The Lancet Neurology, 7 (2008) 779-786.

[28] A. Filali, J.-J. Yaouanc, H. Handel, Toichiometric mono n-functionalization of tetraazamacrocycles via phosphoryl-protected intermediates, Angewandte Chemie International Edition, 30 (1991) 560–561.

[29] J. Du, Z.-Y. Wu, M. Jia, Y.-Z. Li, X.-Y. Wang, Z.-J. Guo, Preparation, characterisation and DNA binding property of a cuii-ptii heterodinuclear complex derived from monosubstituted cyclen, Chinese Journal of Inorganic Chemistry, 24 (2008) 1669-1674.

[30] T. Chen, X. Wang, Y. He, C. Zhang, Z. Wu, K. Liao, J. Wang, Z. Guo, Effects of cyclen and cyclam on zinc(ii)- and copper(ii)-induced amyloid beta-peptide aggregation and neurotoxicity, Inorg Chem, 48 (2009) 5801-5809.

[31] P.K. Smith, R.I. Krohn, G.T. Hermanson, A.K. Mallia, F.H. Gartner, M.D. Provenzano, E.K. Fujimoto, N.M. Goeke, B.J. Olson, D.C. Klenk, Measurement of protein using bicinchoninic acid, Analytical Biochemistry, 150 (1985) 76-85.

[32] L.P. Stabile, A.L.G. Davis, C.T. Gubish, T.M. Hopkins, J.D. Luketich, N. Christie, S. Finkelstein, J.M. Siegfried, Human non-small cell lung tumors and cells derived from normal lung express both estrogen receptor α and β and show biological responses to estrogen, Cancer Research, 62 (2002) 2141-2150.

[33] L.M. Lima, D. Esteban-Gomez, R. Delgado, C. Platas-Iglesias, R. Tripier, Monopicolinate cyclen and cyclam derivatives for stable copper(ii) complexation, Inorg Chem, 51 (2012) 6916-6927.

[34] O.P. Sharma, T.K. Bhat, Dpph antioxidant assay revisited, Food Chemistry, 113 (2009) 1202-1205.

[35] D.P. Reed, G.R. Weisman, 1,4,7,10-tetraazacyclododecane, Org. Synth., 78 (2002) 73.

[36] Bruker, Sadabs, bruker axs inc., Madison, Wisconsin, USA, 2001.

[37] Bruker, Apex2 and saint, bruker axs inc, Madison, Wisconsin, USA, 2007.

[38] G. Sheldrick, A short history of shelx, Acta Crystallographica Section A, 64 (2008) 112-122.

[39] A. OLEX, Complete structure solution, refinement and analysis program: Ov dolomanov, lj bourhis, rj gildea, jak howard, h. Puschmann, J. Appl. Crystallogr, 42 (2009) 339-341.